Slowing down the speed of light using an electromagnetically-induced-transparency mechanism in a modified reservoir

Ronggang Liu
Department of Civil Engineering, Harbin Institute of Technology, Weihai 264209, China

Tong Liu
Aerospace Research Institute of Materials and Processing Technology, Beijing 10076, China

Yingying Wang
Department of Optoelectronic Science, Harbin Institute of Technology, Weihai 264209, China

Yujie Li
School of Materials Science and Engineering, Harbin Institute of Technology, Weihai 264209, China

Bingzheng Gai
Department of Astronautic Science and Mechanics, Harbin Institute of Technology, Harbin 150001, China
(Received 18 April 2017; published 8 November 2017)

We propose an effective method to achieve extremely slow light by using both the mechanism of electromagnetically induced transparency (EIT) and the localization of a coupled cavity waveguide (CCW). Based on quantum mechanics theory and the dispersion relation of a CCW, we derive a group-velocity formula that reveals both the effects of the EIT and CCW. Results show that ultralow light velocity at the order of several meters per second or even static light, could be obtained feasibly. In comparison with the EIT mechanism in a background of vacuum, this proposed method is more effective and realistic to achieve extremely slow light. And it exhibits potential values in the field of light storage.

DOI: 10.1103/PhysRevA.96.053823

I. INTRODUCTION

Slow group velocity of light [1–7] has attracted much attention due to its potential applications in optical buffers [8], low-power optical switches [9], and quantum memories [10]. Generally speaking, there are two important ways to achieve slow light. The first one is to use the narrow spectrum resonance effects of materials to change the light velocity, such as the electromagnetically induced transparency (EIT) mechanism [11], coherent population oscillations (CPO) [12], stimulated Brillouin scattering (SBS) [13], stimulated Raman scattering (SRS) [14], etc. The second way is by means of structural effects of materials; for example, the localization properties of photonic crystals [15,16]. Now, an interesting question is whether the two different mechanisms could cooperate together to get slower light. Here we investigate the slow-light performance from both the EIT and the coupled cavity waveguide (CCW) mechanisms [5]. On one hand, when a Λ-type atomic system is driven by two fields (one is the probe light, and the other is the control light), the probe light propagates with a time delay by tuning the intensity of the control light according to the EIT mechanism. This phenomenon has already been demonstrated experimentally [3,4]. In this case, light can even be trapped in the EIT medium, which is very useful for light storage [17,18]. On the other hand, the density of states (DOS) is very high [19] at the resonance frequencies of a cavity. The DOS is inversely proportional to the group velocity v_g. Hence slow-light velocities can be obtained accordingly [20–23]. One of the most important resonance system for slow light is the CCW fabricated in a photonic crystal [24], in which the rich localization properties have been investigated in our previous work [25]. When light propagates in a multiple CCW, strong localization happens in each cavity, which leads to a rather larger time delay. Our analyses and results show that extremely slow light (several meters per second or even near zero) can be effectively obtained by using this combined mechanism. Since it can be fabricated easily under current technical conditions, a coupling system consisting of a CCW with inner placed atoms becomes a practical optical device, and potentially benefits fields like quantum computation and quantum information [26,27].

II. MODEL AND EQUATIONS

A schematic diagram of the composite EIT and CCW mechanism is shown in Fig. 1. Here CCW is formed by removing an array of rods from a two-dimensional photonic crystal (green circles), as shown in Fig. 1(a). A Λ-type atomic system (blue circle) is embedded in each cavity of the photonic crystal CCW, as shown in Fig. 1(c). Tight-binding cavity mode interacts weakly with the neighboring cavity modes, thus the light can propagate through coupled cavities effectively. The coordinate of the center of the nth cavity is $x = nR$. The levels $|2\rangle$ and $|1\rangle$ are coupled by a probe laser of frequency (Rabi frequency) ω_p (Ω_p). The level $|2\rangle$ is coupled to level $|3\rangle$ by a modified reservoir and a classical standing-wave field aligns along the x direction with frequency ω_c. The Rabi frequency of the coupling field is $\Omega_c \sin(kx)$. Since the transition $|2\rangle$ to $|3\rangle$ is coupled to the structured CCW mode continuum $\{\lambda\}$, we have $\sum_\lambda \to \int d\omega_\lambda \rho(\omega_\lambda)$, where $\rho(\omega_\lambda)$ is the density of states

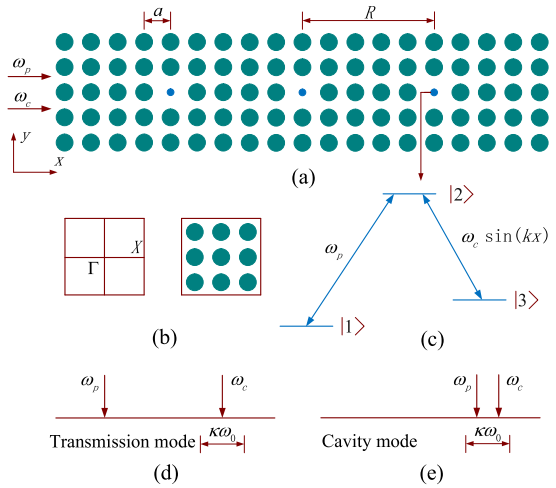

FIG. 1. Schematic sketch of the extremely-slow-light system. (a) The coupled cavity waveguide along the horizontal direction. (b) The irreducible Brillouin zone, and the special points Γ and X. (c) The three-level atomic system in the cavities. (d) A probe light of ω_p in the transmission mode and a localized control light of ω_c. (e) The same as panel (d) except for the probe light is in the localized cavity mode.

[5,23,24] of a CCW. Then the interaction Hamiltonian of the system can be written as

$$H = \sum_i \hbar\omega_i |i\rangle\langle i| - \frac{\hbar}{2}\Big[\Omega_p e^{i(kx-\omega_p t)}|2\rangle\langle 1| + \int d\omega_\lambda A(\omega_\lambda)\rho(\omega_\lambda)\sin(kx)e^{-i\omega_\lambda t}|2\rangle\langle 3| + \text{H.c.}\Big], \quad (1)$$

where

$$A(\omega_\lambda) = L(\omega_\lambda)\sqrt{\Omega_c^2 + (\omega_\lambda - \omega_{23})^2}, \quad (2)$$

and $L(\omega_\lambda)$ is the localization factor of the CCW in the system. The density of states of the CCW is given by

$$\rho(\omega_\lambda) = \frac{1}{\pi R\sqrt{Q^2 - (\omega_\lambda - \omega_0)^2}}, \quad (3)$$

where R is the intercavity distance, $\omega_0 = (1 - \Delta\alpha/2)\Omega$, $Q = \kappa\Omega$, and Ω is the eigenfrequency of a single cavity without coupling. κ is the coupling factor, and $\Delta\alpha$ is a parameter related to the coupled cavity, which is usually much smaller than 1. More details can be found in Ref. [5].

Without loss of generality, we can suppose that the photonic crystal is formed by dielectric cylinders placed in vacuum according to a square lattice. The dielectric constant and the radii of the cylinders are $\epsilon = 8.9$ and $r = 0.2a$, respectively. The lattice constant a is set to be 300 nm, and the intercavity distance $R = 5a$. By using the plane-wave expansion method, we obtain the photonic band structure for the CCW, as shown in Fig. 2. Along the horizontal axis, the in-plane wave vector $\vec{k}$ goes along the edge of the irreducible Brillouin zone, from point Γ to X, where the special points Γ and X correspond to $\vec{k} = 0$ and $\vec{k} = \pi/a\vec{x}$ respectively [see Fig. 1(b)]. Here the results are computed from a coupling factor $\kappa = 0.00242$. Hence there is a very narrow cavity mode with $Q = \kappa\Omega$ for

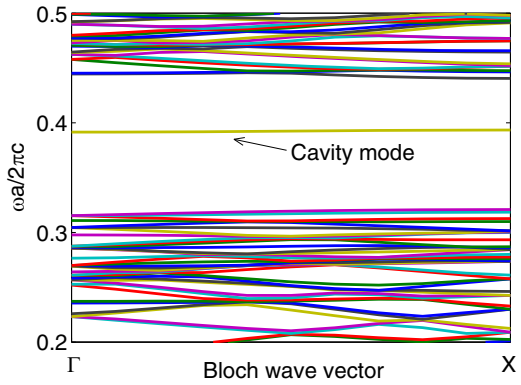

FIG. 2. The photonic band structure for a CCW composed of dielectric columns with the radius $r = 0.2a$, the dielectric constant $\epsilon = 8.9$, and the size of a unit cell is $R = 5a$, as shown in Fig. 1(a).

the structured CCW. One can find that the cavity mode locates within the photonic band gap (see Fig. 2), where the control light works at the corresponding frequency. To investigate light transmission and localization in CCW systems, numerical simulations can be conducted with the finite-difference time-domain (FDTD) method effectively [25,28,29]. Here we define the transmission as $|E_t(f)/E_i(f)|^2$, where $E_t(f)$ is Fourier-transform of transmitted electric fields $E_t(t)$, and $E_i(f)$ is Fourier-transform of incident electric fields $E_i(t)$. Figure 3 gives the transmission curve of the three-cavity system computed by the FDTD method. It is shown that light propagation is prohibited in the x direction between $0.32(2\pi c/a)$ and $0.39(2\pi c/a)$, which can also be observed in Fig. 2. For this case, the result presents clearly a resonance-splitting effect near $\omega = 0.39615(2\pi c/a)$, and the number of peaks just equals the number of cavities, as shown in the inset to Fig. 3. This splitting property excellently mimics a multiple photonic quantum well system [25]. Furthermore, one can see some effective traveling transmission modes occur between $0.3(2\pi c/a)$ and $0.32(2\pi c/a)$, as shown in Fig. 3. When the frequency ω is confined to $0.39615(2\pi c/a)$, it is found that strong localized states occur in odd-indexed cavities, as depicted in Fig. 4. All these phenomena are very similar to the phenomenon that occurs in the one-dimensional case [25]. It will be demonstrated below that the strong localization of the

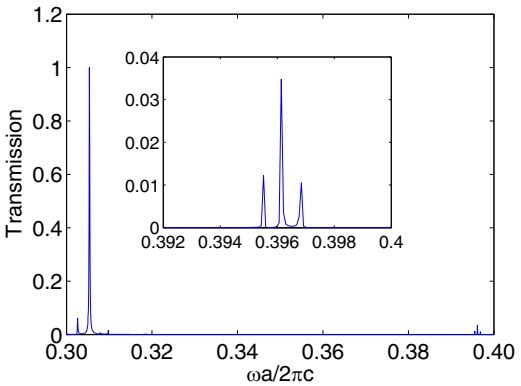

FIG. 3. Transmission spectrum of a three-cavity CCW.

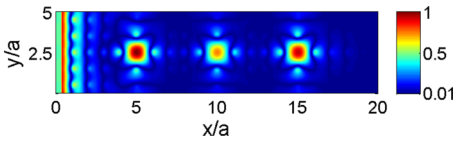

FIG. 4. Field distribution (normalized with the maximum of the electric-field density) of incident light with $\omega = 0.39615(2\pi c/a)$ in a three-cavity CCW, where both x and y coordinates are scaled by the the lattice constant a.

cavity modes can contribute to the achievement of extremely slow light.

To achieve the precise localization of atoms [30–34] into the cavity, here we use a subwavelength atomic localization technology. We presented a scheme for subwavelength atom localization via manipulation of Raman gain process [30]. Our strategy here is to localize atomic position from the susceptibility of the system at the probe field frequency and simultaneously obtaining an ultralow light velocity. It is very interesting that the information about the atomic position is just described with the imaginary part of the susceptibility, and low light velocity can be related to the real part of the susceptibility. Since the susceptibility is determined by the density-matrix elements, the equations of motion for the density-matrix elements are then given by

$$\dot{\rho}_{21} = \frac{i}{2}\Omega_p e^{i(kx-\omega_p t)}(\rho_{11}-\rho_{22}) + \frac{i}{2}B\sin(kx)e^{-i\omega_c t}\rho_{31} - (\gamma + i\omega_{21})\rho_{21}, \tag{4}$$

$$\dot{\rho}_{23} = \frac{i}{2}\Omega_p e^{i(kx-\omega_p t)}\rho_{13} + \frac{i}{2}B\sin(kx)e^{-i\omega_c t}(\rho_{33}-\rho_{22}) - (\gamma_0 + i\omega_{23})\rho_{23}, \tag{5}$$

$$\dot{\rho}_{31} = -\frac{i}{2}\Omega_p e^{i(kx-\omega_p t)}\rho_{32} + \frac{i}{2}B\sin(kx)e^{-i\omega_c t}\rho_{21} - i\omega_{31}\rho_{31}. \tag{6}$$

The off-diagonal decay rates for ρ_{21} and ρ_{23} are denoted by γ and γ_0, respectively. The parameter B can be given by

$$B = \frac{1}{\pi R}\int_{\omega_0-\frac{\xi}{2}Q}^{\omega_0+\frac{\xi}{2}Q} d\omega L(\omega)\sqrt{\frac{\Omega_c^2+(\omega-\omega_{23})^2}{Q^2-(\omega-\omega_0)^2}}, \tag{7}$$

where ξ is the linewidth factor of the coupling laser. Because integration interval is very narrow, the localization factor $L(\omega)$ can be changed with the frequency weakly, and $\omega_0 \approx \omega_{23}$, we have $B \approx \frac{L\xi}{\pi R}\Omega_c$. The localization factor L can be adjusted by changing the properties of cavities and the intercavity distance. For example, when L has a 10^3 order, ξ has a 10^{-6} order. Using the relations $P(z,t) = \epsilon_0\chi E_0$, $p(z,t) = 2|\vec{\mu}_{21}|\rho_{21}e^{-i(kx-\omega_p t)}$, and $P(z,t) = N_a p(z,t)$, where $p(z,t)$ is the slowly varying complex polarization, N_a is the density of doping atoms, $|\vec{\mu}_{21}|$ is the magnitude of the dipole-matrix element between $|2\rangle$ and $|1\rangle$, and E_0 is the amplitude of the probe light, the nonlinear Raman susceptibility [30] can be given by

$$\chi = \frac{2N_a|\vec{\mu}_{21}|^2}{\hbar\epsilon_0\Omega_p}\rho_{21}e^{-i(kx-\omega_p t)}. \tag{8}$$

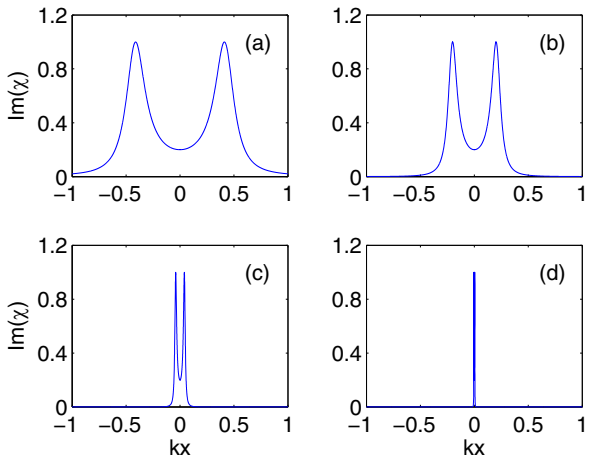

FIG. 5. Im(χ) as a function of kx for the parameters $\Delta = 2\gamma$: (a) $B = 10\gamma$, (b) $B = 20\gamma$, (c) $B = 100\gamma$, and (d) $B = 1000\gamma$.

Because the atoms are initially in the ground level $|1\rangle$, $\rho_{11}^{(0)} = 1$, $\rho_{22}^{(0)} = \rho_{33}^{(0)} = \rho_{32}^{(0)} = 0$. Using Eq. (8), the complex susceptibility χ reads

$$\chi = \frac{N_a|\vec{\mu}_{21}|^2\Delta[i\gamma\Delta + \Delta^2 - B^2\sin^2(kx)/4]}{\epsilon_0\hbar[(\Delta^2 - B^2\sin^2(kx)/4)^2 + \Delta^2\gamma^2]}. \tag{9}$$

We know that the Raman gain is directly proportional to the imaginary part of the susceptibility. A subwavelength atom localization through the Raman gain process will be considered in the following section.

III. RESULTS AND DISCUSSIONS

The maxima of the imaginary part of the susceptibility are found when the probe-light detuning satisfies the equation

$$\Delta = \pm\frac{B}{2}\sin(kx). \tag{10}$$

This means that the maxima are located at

$$kx = \pm\sin^{-1}(2\Delta/B) + n\pi, \tag{11}$$

where n is an integer. Therefore, the degree of localization depends on the detuning Δ and the parameter B. In Fig. 5, we present the results for the position probability distribution with the influence of the coupling-field strength in a CCW. The localization becomes more pronounced with B increasing as shown in Figs. 5(a)–5(d). The full width at half maximum (FWHM) of the higher peak in Fig. 5(b) can easily be obtained numerically and it comes out to be 0.105, which means the localization is larger than $\lambda/50$. For the given detuning Δ, high-precision and high-resolution localization patterns can be obtained by adjusting B. We know that the strong localization occurs in the CCW cavity, in which the parameter B of the system is significantly dependent on geometrical characteristics of the system. The high-precision atom localization can originate from quantum interference, and furthermore the behavior relies remarkably on the strong coupling effect between an atom and a CCW. A similar phenomenon appears in Ref. [35], in which the fluorescence line near the quenching point can be enhanced greatly.

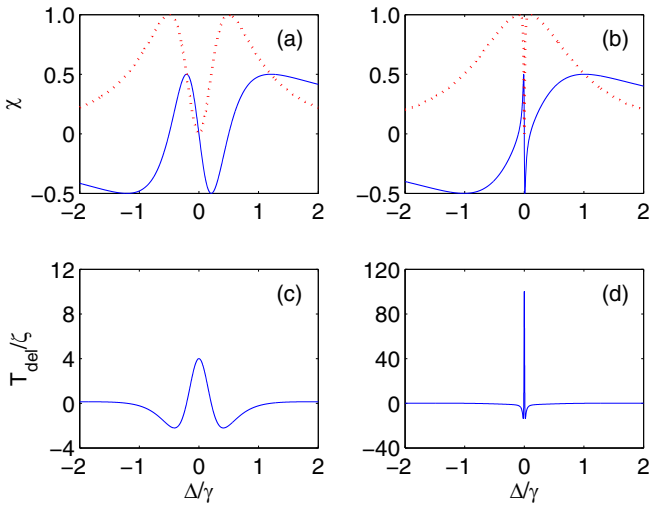

FIG. 6. (a), (b) Imaginary (red dashed line) and real (blue solid line) parts of the complex polarizability χ changing with the detuning Δ: (a) $B = \gamma$, (b) $B = 0.2\gamma$. (c), (d) Delay time per unit length, $T_{\rm del}$, as a function of the detuning Δ, where $\zeta = N_a|\vec{\mu}_{21}|^2/\epsilon_0\hbar\gamma^2$. (c) $B = \gamma$. (d) $B = 0.2\gamma$.

In this paper, the control light is set to be in the localized cavity modes; the probe light, however, can be in a travelling transmission mode or a localized cavity mode, as shown in Figs. 1(d) and 1(e). These two cases are very different and will be investigated respectively in the following. When the probe light is in a transmission mode with a typical normalized frequency, for example, $\omega_p = 0.306(2\pi c/a)$ (see Fig. 3), the CCW can be approximately regarded as a homogeneous bulk medium. Therefore, the group velocity of the probe light will be reduced due to the large effective dielectric constant. According to the definition, we derive the group velocity of the probe light as

$$v_g^{\rm tra} = \frac{c}{n_p + c\frac{\partial {\rm Re}(\chi)}{\partial \omega_p}}, \tag{12}$$

where n_p is the average refractive index, and then the delay time per unit length is given by

$$T_{\rm del} = \frac{\partial {\rm Re}(\chi)}{\partial \omega_p}. \tag{13}$$

When the EIT mechanism is absent, which means the number of EIT atoms tends to be zero, the denominator of Eq. (12) approaches n_p. Then the group velocity of the probe light v_g tends to be c/n_p, which is the group velocity in the bulk photonic crystal. When $\frac{\partial {\rm Re}(\chi)}{\partial \omega_p} \gg 1$, the group velocity v_g^{tra} is much smaller than c/n_p, and slow light is obtained by the coupling mechanism. This is also demonstrated from the polarizability and delay time (shown in Fig. 6). At zero detuning, for different values of the coupling constant B, the absorption vanishes and the dispersion slope is very steep as shown in Figs. 6(a) and 6(b). For the given coupling constant $B = \gamma$, a large delay time occurs near $\Delta = 0$, as illustrated in Fig. 6(c). One has to keep in mind, however, a large delay time occurs at $\Delta = 0$ when the control beam is strongly coupled to structured CCW and the probe beam resonates with the transition frequency between level $|2\rangle$ and level $|1\rangle$. Therefore,

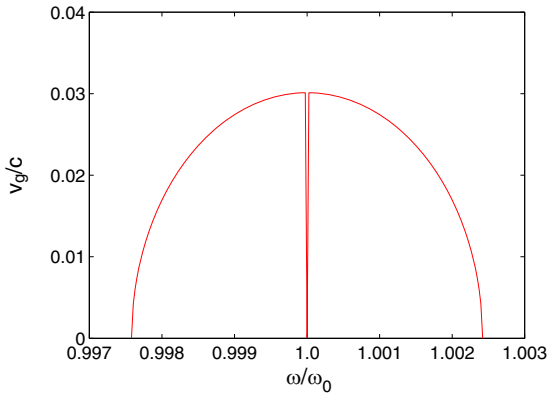

FIG. 7. Changes of the group velocity $v_g^{\rm cav}$ with ω/ω_0, $B = 20\gamma$, where the probe light is in the cavity mode as shown in Fig. 1(e).

the coupling effect contributes a lot, and when $B = 0.2\gamma$ a very large delay time at $\Delta = 0$ is shown in Fig. 6(d). That is, in order to have a larger delay time T_{del}, the coupling constant B should adopt a smaller value. One can infer from Eq. (7) that a narrower linewidth factor ξ means a larger delay time. This interesting phenomenon reveals that the slow light can be achieved by tuning the linewidth of the coupling laser effectively. It means a laser with narrower linewidth enhances the coupling effect between atoms and cavities of the system. Now, we consider the case shown in Fig. 1(e), i.e., the probe light is also in localized cavity modes. Using the group velocity of the probe light $v_g^{-1} = \pi\rho(\omega)$ in CCW, by means of the same method, we derive the formula of $v_g^{\rm cav}$ in this case, which reads

$$v_g^{\rm cav} = \frac{R\sqrt{Q^2 - (\omega - \omega_0)^2}}{1 + \Gamma}, \tag{14}$$

where

$$\Gamma = \frac{c}{n_p}\frac{\partial {\rm Re}(\chi)}{\partial \omega_p}. \tag{15}$$

To understand the group velocity quantitatively, we calculate the change of $v_g^{\rm cav}$ with ω/ω_0. The results are plotted in Fig. 7. When $\Gamma \to 0$, $v_g^{\rm cav}$ takes the form of $R[Q^2 - (\omega - \omega_0)^2]^{1/2}$, which means $v_g^{\rm tra}$ can be reduced exactly to the group velocity of the CCW when EIT is absent. When a slow-light performance is produced from both the EIT and the coupled cavity waveguide (CCW) mechanisms v_g, tends to zero sharply at $\omega/\omega_0 = 1$. This means the working frequency of the extremely slow light is just the eigenfrequency of a single cavity Ω. The strong coupling effect occurs in cavity-EIT with a single atom, in which the weak probe field is coupled to the single cavity mode and then propagates without absorption at a reduced group velocity compared to in vacuum. The results show that the two different mechanisms could cooperate together to trap light at the center of the guide mode. It is also noticed that ultralow group velocity occurs at the edges of the guide mode; for example, near $\omega/\omega_0 = 0.9977$ or $\omega/\omega_0 = 1.0027$. This means storage of light at the frequencies of the band-edge modes could be accomplished. Comparing Eqs. (12) and (14), one can conclude that the localized cavity mode is much more effective than the transmission mode for achieving extremely slow light. These analyses imply that the group-velocity delays induced by the EIT mechanism and the

CCW can be superimposed. Furthermore, when $B = 20\gamma$ is set, the atomic localization is larger than $\lambda/50$ from Fig. 5(b). Thus, a large group-velocity delay with the high-precision atom localization can be achieved in the system effectively.

Considering the ability to achieve extremely slow light is measured by the maximum achievable fractional delay (also known as the delay-bandwidth product), to limit the pulse distortion, a realistic system requires at least a delay-bandwidth product of 100. Fortunately, the EIT mechanism in the environment of coupled cavity structure can reach the value by using a highly absorptive material in vapors [3,36], in which strong localization effects of the coupled cavity can help pump significant laser power to saturate the EIT transition. Furthermore, as a general technique, an artificial inhomogeneous broadening has been proposed to solve the delay-bandwidth limitation in solid-state room-temperature slow light [36].

IV. CONCLUSION

We have investigated the group velocity of light under the EIT mechanism in the environment of coupled cavity structure. It is shown that, for our considered system, atom localization in the subwavelength domain can be improved significantly due to the quantum interference effect. High-precision and high-resolution atom localization pave the way to achieve a large group-velocity delay. Furthermore, analytical formulas of the group velocities are derived, and they reduce exactly to the values for transmission in the background medium (the coupled cavity waveguide) when the EIT mechanism is absent. Due to the strong localization of the coupled cavity structure, the EIT effect is greatly enhanced, and extremely slow light (several meters per second or static light at moderate parameters given in this paper) is obtained. The superposition of the EIT mechanism and localization of cavities provides an effective and realistic way to acquire slow light and may find potential applications in optical storage and optical information processing.

ACKNOWLEDGMENTS

The authors wish to thank Professor Weiqiang Ding for useful discussions.

[1] M. Bajcsy, S. Hofferberth, V. Balic, T. Peyronel, M. Hafezi, A. S. Zibrov, V. Vuletic, and M. D. Lukin, Phys. Rev. Lett. **102**, 203902 (2009).
[2] T. Kampfrath, D. M. Beggs, T. P. White, A. Melloni, T. F. Krauss, and L. Kuipers, Phys. Rev. A **81**, 043837 (2010).
[3] L. V. Hau, S. E. Harris, Z. Dutton, and C. H. Behroozi, Nature (London) **397**, 594 (1999).
[4] C. Liu, Z. Dutton, C. H. Behroozi, and L. V. Hau, Nature (London) **409**, 490 (2001).
[5] A. Yariv, Y. Xu, R. K. Lee, and A. Scherer, Opt. Lett. **24**, 711 (1999).
[6] M. Bayindir and E. Ozbay, Phys. Rev. B **62**, R2247 (2000).
[7] Y. Terada, K. Miyasaka, H. Ito, and T. Baba, Opt. Lett. **41**, 289 (2016).
[8] J. Scheuer and M. S. Shahriar, Opt. Lett. **38**, 3534 (2013).
[9] K. Lee, J. Park, J. Lee, and K. Yang, Opt. Lett. **40**, 1022 (2015).
[10] D. T. Stack, P. J. Lee, and Q. Quraishi, Opt. Express **23**, 6822 (2015).
[11] M. O. Scully and M. S. Zubairy, *Quantum Optics* (Cambridge University Press, Cambridge, 1999).
[12] G. M. Gehring, A. Schweinsberg, C. Barsi, N. Kostinski, and R. W. Boyd, Science **312**, 895 (2006).
[13] Y. Okawachi, M. S. Bigelow, J. E. Sharping, Z. Zhu, A. Schweinsberg, D. J. Gauthier, R. W. Boyd, and A. L. Gaeta, Phys. Rev. Lett. **94**, 153902 (2005).
[14] J. E. Sharping, Y. Okawachi, and A. L. Gaeta, Opt. Express **13**, 6092 (2005).
[15] Y. A. Vlasov, M. O'boyle, H. F. Hamann, and S. J. McNab, Nature (London) **438**, 65 (2005).
[16] T. Baba, Nat. Photonics **2**, 465 (2008).
[17] M. Fleischhauer and M. D. Lukin, Phys. Rev. Lett. **84**, 5094 (2000).
[18] M. Fleischhauer and M. D. Lukin, Phys. Rev. A **65**, 022314 (2002).
[19] R. Liu, Opt. Commun. **319**, 147 (2014).
[20] K. Sakoda and K. Ohtaka, Phys. Rev. B **54**, 5742 (1996).
[21] A. Imhof, W. L. Vos, R. Sprik, and A. Lagendijk, Phys. Rev. Lett. **83**, 2942 (1999).
[22] J. G. Pedersen, S. Xiao, and N. A. Mortensen, Phys. Rev. B **78**, 153101 (2008).
[23] D. Petrosyan and G. Kurizki, Phys. Rev. A **64**, 023810 (2001).
[24] V. Yannopapas, J. Opt. B: Quantum Semiclassical Opt. **6**, 283 (2004).
[25] R. Liu and B. Gai, J. Opt. Soc. Am. B **24**, 2369 (2007).
[26] M. A. Nielsen and I. L. Chuang, *Quantum Computation and Quantum Information* (Cambridge University Press, Cambridge, 2000).
[27] J. X. Wu, C. Zhu, and Y. P. Yang, Opt. Lett. **40**, 4975 (2015).
[28] D. M. Sullivan, *Electromagnetic Simulation Using the FDTD Method* (IEEE Press, New York, 2000).
[29] A. Taflove and S. C. Hagness, *Computational Electrodynamics: The Finite-Difference Time-Domain Method*, 3rd ed. (Artech House, Norwood, 2005).
[30] S. Qamar, A. Mehmood, and S. Qamar, Phys. Rev. A **79**, 033848 (2009).
[31] E. Paspalakis and P. L. Knight, Phys. Rev. A **63**, 065802 (2001).
[32] C. Ding, J. Li, Z. Zhan, and X. Yang, Phys. Rev. A **83**, 063834 (2011).
[33] R. Wan, J. Kou, Li. Jiang, Y. Jiang, and J. Gao, J. Opt. Soc. Am. B **28**, 10 (2011).
[34] R. Liu, Int. J. Theor. Phys. **54**, 2830 (2015).
[35] R. Liu and T. Liu, Opt. Quantum Electron. **48**, 186 (2016).
[36] Z. Deng, D.-K. Qing, P. Hemmer, C. H. Raymond Ooi, M. S. Zubairy, and M. O. Scully, Phys. Rev. Lett. **96**, 023602 (2006).